Historic storms and the hidden value of coastal wetlands for nature-based flood defence

Zhu, Zhenchang; Vuik, Vincent; Visser, Paul J.; Soens, Tim; van Wesenbeeck, Bregje; van de Koppel, Johan; Jonkman, Sebastiaan N.; Temmerman, Stijn; Bouma, Tjeerd J.

DOI
10.1038/s41893-020-0556-z

Publication date
2020

Document Version
Final published version

Published in
Nature Sustainability

nature sustainability

ARTICLES

https://doi.org/10.1038/s41893-020-0556-z

Check for updates

Historic storms and the hidden value of coastal wetlands for nature-based flood defence

Zhenchang Zhu[1,2,3]✉, Vincent Vuik[4,5], Paul J. Visser[4], Tim Soens[6], Bregje van Wesenbeeck[7], Johan van de Koppel[1], Sebastiaan N. Jonkman[4], Stijn Temmerman[8] and Tjeerd J. Bouma[1,9,10]

Global change amplifies coastal flood risks and motivates a paradigm shift towards nature-based coastal defence, where engineered structures are supplemented with coastal wetlands such as saltmarshes. Although experiments and models indicate that such natural defences can attenuate storm waves, there is still limited field evidence on how much they add safety to engineered structures during severe storms. Using well-documented historic data from the 1717 and 1953 flood disasters in Northwest Europe, we show that saltmarshes can reduce both the chance and impact of the breaching of engineered defences. Historic lessons also reveal a key but unrecognized natural flood defence mechanism: saltmarshes lower flood magnitude by confining breach size when engineered defences have failed, which is shown to be highly effective even with long-term sea level rise. These findings provide new insights into the mechanisms and benefits of nature-based mitigation of flood hazards, and should stimulate the development of novel safety designs that smartly harness different natural coastal defence functions.

Coastal flood disasters are responsible for extensive casualties and billions of dollars of damage to coastal communities[1,2]. Dramatic examples include the floods induced by Hurricane Katrina (New Orleans, 2005), causing 1,833 deaths and US$108 billion of damage[3], and Typhoon Haiyan (Philippines, 2013), resulting in over 6,000 deaths and US$14 billion of losses[4]. Also, in temperate climate zones, storm surges can have devastating effects. For instance, 1,836 people died in the Netherlands during the 1953 North Sea flood[5,6] and more than 11,000 people were killed during the 1717 Christmas flood in the Netherlands, Germany and Denmark[7,8]. To mitigate the enhanced coastal flood risks due to sea level rise[9], the possible increase in storm intensity[10], land subsidence[11] and population growth[12], it has been increasingly proposed that innovative, nature-based solutions be implemented that supplement conventional engineered structures (for example, dykes, seawalls and levees) with natural or constructed coastal wetlands such as saltmarshes and mangroves[1,13–15].

In many cases, combining engineered structures and coastal wetlands to create so-called 'hybrid' solutions is considered to provide a more sustainable sea defence than engineered defences alone[13,14]. Coastal wetlands not only dissipate wave impacts and reduce erosion risks to engineered structures[16,17], but they also build up with sea level rise by accumulating sediments in places where sediment supply is sufficient[18,19]. Furthermore, they provide additional valuable ecosystem services, such as carbon storage, fisheries production and biodiversity conservation[17]. Experiments and models indicate that coastal wetlands can reduce the impacts of storm waves[20–22]. Although reduced wave loads are expected to lower the chances of overtopping and breaching of engineered defences[16,23], there is still limited field evidence on how much coastal wetlands can add safety to engineered structures during extreme conditions. Such a knowledge gap poses a major uncertainty in the actual value of and need for nature-based flood protection that reinforces existing engineered defences with coastal wetlands. This hampers the widespread application of such hybrid flood defences[24]. Here, we derive empirical evidence on both the effectiveness and the underlying mechanisms of nature-based mitigation of coastal flooding from two well-known and well-documented historic flood disasters in Northwest Europe, namely those of 1717 and 1953. We reveal that saltmarshes have displayed effectiveness in reducing both the occurrence and impact of dyke breaching during extreme historic storms that killed tens of thousands of people. Beyond wave attenuation, historic lessons also reveal a highly relevant but overlooked function of wetlands for protecting humans against coastal flooding.

Saltmarshes as complements to engineered defences

The historic records of a major storm surge in December 1717 (locally named the 1717 Christmas flood) demonstrate the protective role of saltmarshes in reducing the chance of dyke breaching. This approximately 1-in-300-year storm breached hundreds of dykes along the Dutch, German and Danish Wadden Sea coast, resulting in the most deadly flood disaster in the recorded history of the North Sea area[7]. An historic map (Fig. 1a) and reports[25] document detailed information on the distribution and dimensions of dyke breaches (Supplementary Table 1) and the presence of saltmarshes along the Dutch coast. Our analysis of this map shows a notable decreasing trend in the chance of dyke breaching with increasing marsh width in front (Fig. 1b). For dyke sections behind mudflats and the adjacent narrow marshes (marsh width class C1: 0–200 m; Fig. 1a), 15 breaches occurred along a 2.5-km stretch of dyke, including three 'mega breaches' where sections of dyke completely disappeared (Fig. 1a). By contrast, ten breaches occurred

[1]Department of Estuarine and Delta Systems, Royal Netherlands Institute for Sea Research and Utrecht University, Yerseke, the Netherlands. [2]Guangdong Provincial Key Laboratory of Water Quality Improvement and Ecological Restoration for Watersheds, Institute of Environmental and Ecological Engineering, Guangdong University of Technology, Guangzhou, China. [3]Southern Marine Science and Engineering Guangdong Laboratory (Guangzhou), Guangzhou, China. [4]Delft University of Technology, Civil Engineering and Geosciences, Delft, the Netherlands. [5]HKV Consultants, Lelystad, the Netherlands. [6]Department of History, University of Antwerp, Antwerp, Belgium. [7]Deltares, Delft, the Netherlands. [8]Ecosystem Management Research Group, University of Antwerp, Wilrijk, Belgium. [9]Faculty of Geosciences, Department of Physical Geography, Utrecht University, Utrecht, the Netherlands. [10]Building with Nature group, HZ University of Applied Sciences, Vlissingen, the Netherlands. ✉e-mail: zhenchang.zhu@nioz.nl

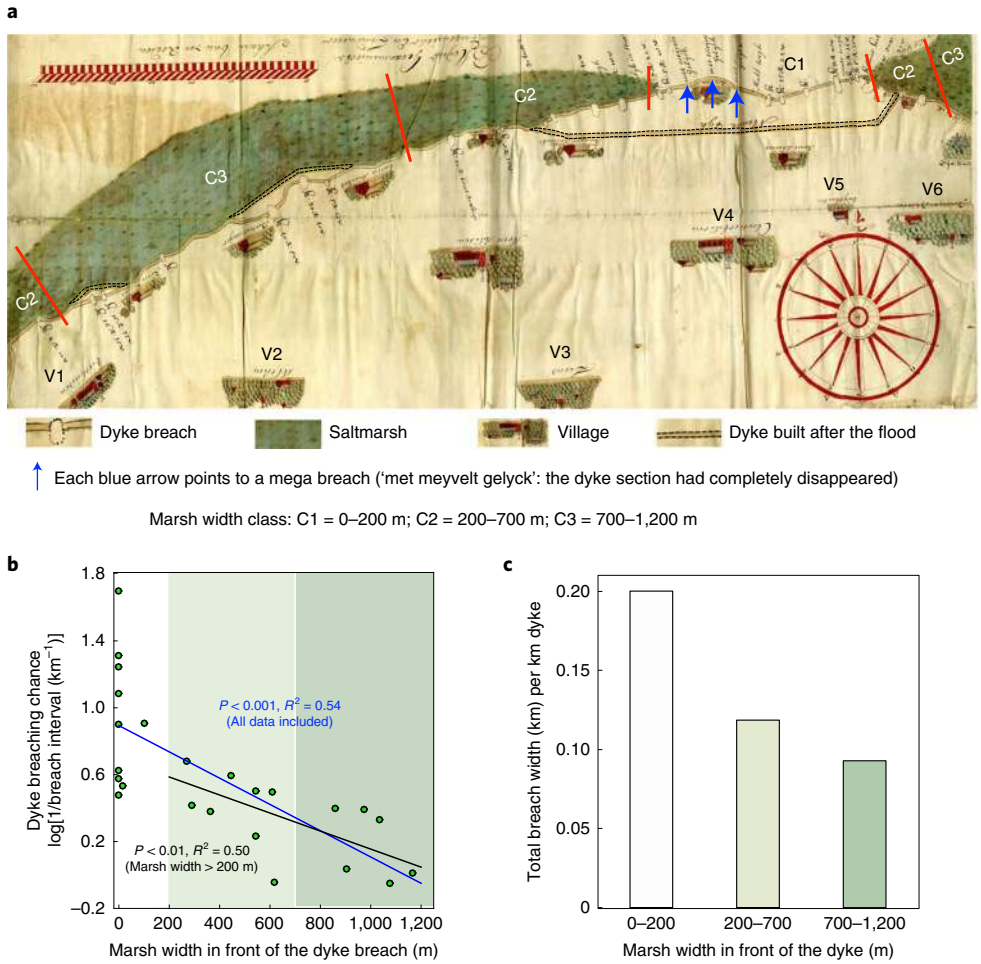

Fig. 1 | Analysis of dyke breach records during the 1717 Christmas flood. a, An historic map recording dyke breaches along the Wadden Sea coast of the Dutch province of Groningen during the 1717 flood. **b**, A linear regression analysis between marsh width and chance of dyke breaching measured as the inverse of the interval between breaches. The data were log transformed to better fit the normal distribution. **c**, Fraction of breached dykes (that is, the total breach width per unit dyke length) for different classes of marsh width. Map adapted with permission from Historisch archief, Waterschap Amstel, Gooi en Vecht, Amsterdam (file number 020478).

along the 4.1-km dyke sections behind wide marshes (marsh width class C2: 200–700 m; Fig. 1a) and there were only six breaches along the 4.9-km dyke sections behind very wide saltmarshes (marsh width class C3: 700–1,200 m; Fig. 1a). No 'mega breaches' were found behind saltmarsh foreshores, even though dyke sections there were 0.8–1.5 m lower and 9.8–16.8 m narrower than those behind bare tidal flats (Supplementary Table 2). Nevertheless, the total breach width (per unit dyke length) of the dyke sections behind mudflats and adjacent narrow marshes was noticeably higher than that of the dyke sections with wide marshes (>200 m) in front (Fig. 1c), even if we regarded the three 'mega breaches' as average ones.

Further analysis indicates that the remarkable differences in breaching probability for different dyke sections is primarily a result of wave reduction by the saltmarsh rather than distinct wave forcing along the shoreline. A map from the 1740s displays uniform tidal flats fronting the marshes of the considered area similar to the current configuration (Fig. 2). This implies no large spatial differences in water depths and incoming waves at the marsh edge during the 1717 storm, as storm waves are limited in height by the water depth in the shallow Wadden Sea. Unfortunately, the lack of related historic data prevents the reconstruction of tidal and wave conditions during the 1717 storm. Nevertheless, detailed model simulations (see Methods for details) for the present-day coast of this district confirm that water levels and wave heights during severe storm surges are comparable along the shoreline where there are uniform tidal flats, regardless of marsh width (Supplementary Fig. 1). Dyke sections that have no marsh in front may have tidal flats with a very different topography as compared with other dyke sections with marsh foreshores. Therefore, we conducted an additional analysis by excluding dyke sections without marsh foreshores to avoid this uncertainty. Interestingly, the correlation between breach interval and marsh width remains significant ($P < 0.01$, Fig. 1b), suggesting that marsh width affected the probability of dyke breaching during the 1717 storm.

This is further supported by recent (2015 and 2017) storm observations for a wave-exposed marsh in the same region (Fig. 3a). The data clearly reveal that wave run-up height on the dyke drops notably with increasing marsh width in front, as a result of wave attenuation by the saltmarsh system (Fig. 3b,c). Lowered wave run-up reduces the chance of wave overtopping and thus dyke breaching[16,23]. Although these two recent storm surges (1-in-5 year) were orders of magnitude different from the 1717 flood, the data show the most extreme wave conditions ever reported so far for saltmarsh shores (Supplementary Table 3). Moreover, these data provide strong empirical evidence for wider saltmarshes being more efficient in mitigating storm waves. Recent modelling work confirmed

Fig. 2 | Maps of the Wadden Sea coast in the region considered in this study. a, An historic map showing the coastal geometry of the Dutch Wadden Sea area in the 1740s. The marshes (green) in the region depicted in Fig. 1a (within the red square) were bordered by uniform tidal flats (the grey area, 'Het groninger Wadt'). **b**, A map showing the present-day geometry of the Dutch Wadden Sea coast. The marshes (green) in the same region as shown in **a** are also surrounded by uniform tidal flats (the brown area). The bathymetry data (shown as the bed level) were obtained by Rijkswaterstaat (Dutch Ministry of Infrastructure and the Environment) in 2012. Credit: A.N., Groninger Archieven — NL-GnGRA_817_1069 (map in **a**); Google Earth, Landsat/Copernicus (Landsat image).

that even during extreme water levels (up to 1-in-10,000 year), saltmarshes are effective for wave attenuation and their efficiency depends on marsh width[26]. Additionally, bed level measurements showed effective sediment stabilization by marsh vegetation during the 2017 storm. The marsh was stable, whereas strong erosion was observed on the nearby bare mudflat (Fig. 3b), which is in line with laboratory flume experiments showing limited erosion underneath a saltmarsh canopy during simulated extreme storm conditions[20,27].

Hidden value of saltmarshes for flood protection

Evidence form the 1953 North Sea flood further highlights a generally overlooked safety benefit of the higher elevated and stable saltmarsh foreshore: it limits breach dimensions when the dyke fails. This approximately 1-in-250-year storm surge resulted in 520 breaches on the primary dykes (including both wave-exposed and wave-sheltered sites) in the Netherlands[5]. Our analyses of all these breaches show that breaches of the dyke sections with stable marsh foreshores (saltmarshes or outer polders) had limited breach development. In this case, the breach depth (height at the upstream edge) was restricted to the bed level of the marsh foreshore (number of breaches implicated, $n = 166$) or to above the bed level of the marsh foreshore ($n = 94$) when revetments on the outer slopes of the primary dykes were also present. By contrast, deep breaches ($n = 78$) developed in dykes behind open water and bare tidal flats (or in a few cases very narrow marshes) as they were highly erodible, unless there were solid berm structures or revetments on the outer dyke slopes that restricted breach development ($n = 182$).

A typical example is found along the former Dutch estuary Haringvliet, where two nearby breaches on the same dyke differed greatly in size (Fig. 4a), despite originating at about the same time. The one behind the lower elevated mudflat developed into a much deeper and wider breach than the breach behind the higher elevated marsh[5] (Fig. 4a). The width of both breaches was reached after the first tide (that is, 70 and 30 m, respectively)[5]. The breach behind the mudflat became very deep after the second tide, which was 5.5 m lower than the polder level (the latter being at 0 m with respect to mean sea level (MSL))[5]. In contrast, there was no further breach development for the one behind the marsh, as the height of

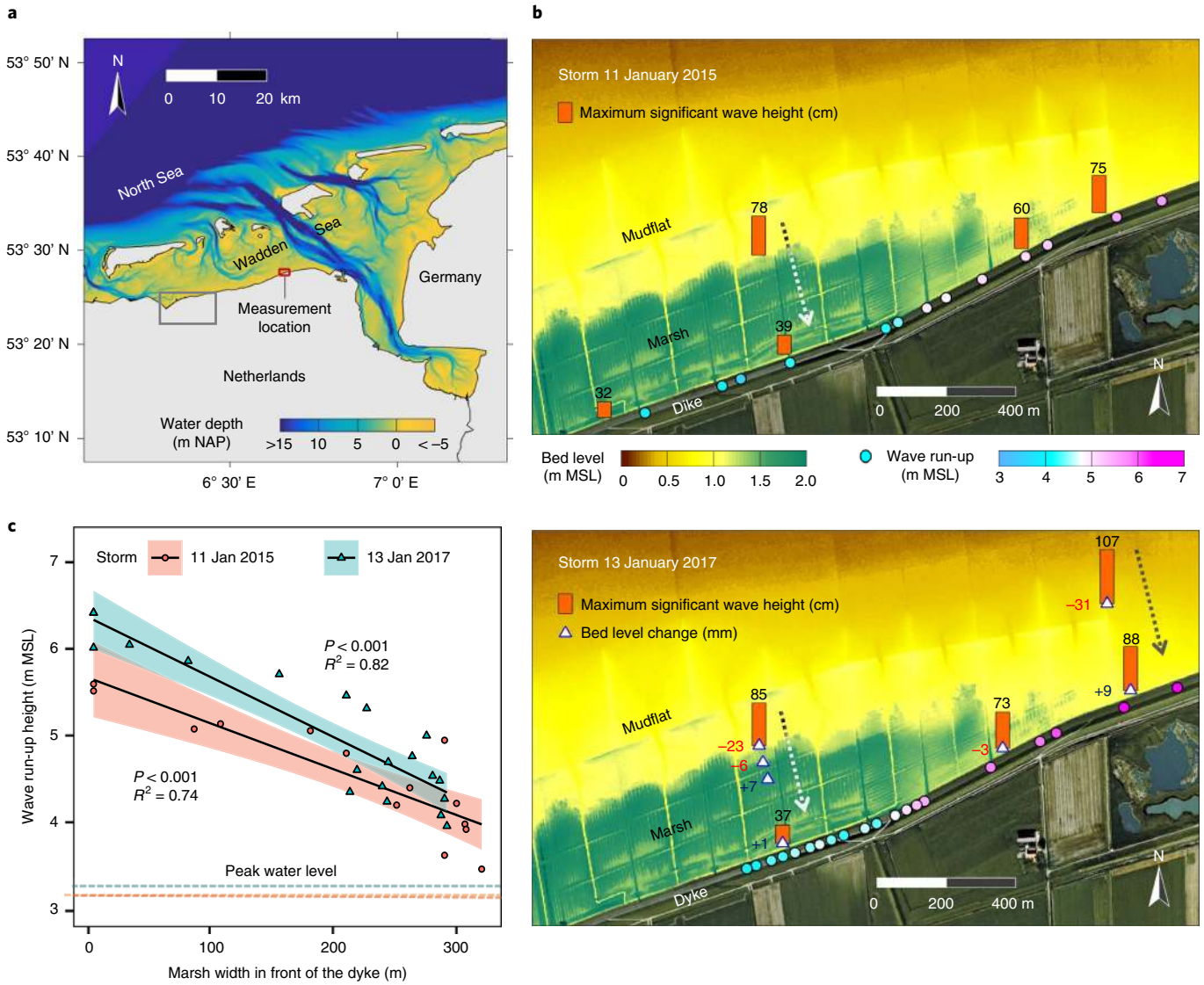

Fig. 3 | Recent storm observations for a wave-exposed marsh in the Wadden Sea. a, Geographic position of the storm observation site (red rectangle). The area depicted in the historic map shown in Fig. 1a (grey rectangle) is to the west of this site. **b**, Maximum significant wave heights, bed level changes at multiple stations (marked with triangles) in front of the dyke and wave run-up height (m above MSL) on the dyke observed during the two storms. **c**, Wave run-up height on the dyke decreased markedly with increasing width of the saltmarsh foreshore.

the marsh platform prevented water movement during subsequent days[5]. The presence of a stable saltmarsh limited the water depth at the upstream edge of the breach (Fig. 4b), thereby resulting in lower flow velocity and slower breach widening as compared with the dyke breach behind the mudflat or open water[23]. Subsequent calculations for these two typical breach types (see Methods for details) demonstrate that shallow breaches behind saltmarsh foreshores discharge much less water than deep breaches that occur in dykes bordered by the lower elevated tidal flats (Fig. 4c), even if we conservatively assume no delayed breaching process and no reduced breach width behind saltmarshes. Reduced inflow discharge consequently leads to slower water level rise and lower inundation depth in the land area behind the dyke (Fig. 4d), which can relieve property damage and casualties in flood disasters[28]. Thus, reduced breach depth by the generally higher elevated saltmarsh foreshores can greatly mitigate flood losses.

Further analysis of the two typical dyke breach types (Fig. 4a) illustrates that the relative advantage of saltmarsh foreshores over tidal flats in mitigating flood impacts is more pronounced with greater breach width, and this will become increasingly prominent with future sea level rise. For the same tidal and storm surge height relative to mean sea level, sea level rise is expected to cause higher water depth on the sea side of the dyke with non-adapted tidal flats. By contrast, it remains unchanged for an adapted saltmarsh foreshore that builds up elevation with a rising sea[15,18,19] (Fig. 5a). Rising sea levels can greatly raise the expected fatality rate (that is, the percentage of lives lost) for a dyke breach behind non-adapted bare tidal flats, whereas the self-adapting saltmarsh foreshore constantly limits the loss of lives to a much lower level (Fig. 5b). The differences between the fatality rates for the two breaching types are large, even with highly conservative comparisons, in which it is assumed that there is no delayed breaching process and no reduced breach width behind saltmarshes. Taking the case of a total breach width of 200 m as an example, a rise in sea level by 50 cm nearly triples the expected fatality rate (from 4.5 to 12.1%) for the scenario with non-adapted tidal flats, whereas it increases slightly (from 0.7 to 1%) for the nature-based scenario with saltmarsh foreshores (Fig. 5b). Additional analysis shows that even if tidal flats can adapt in

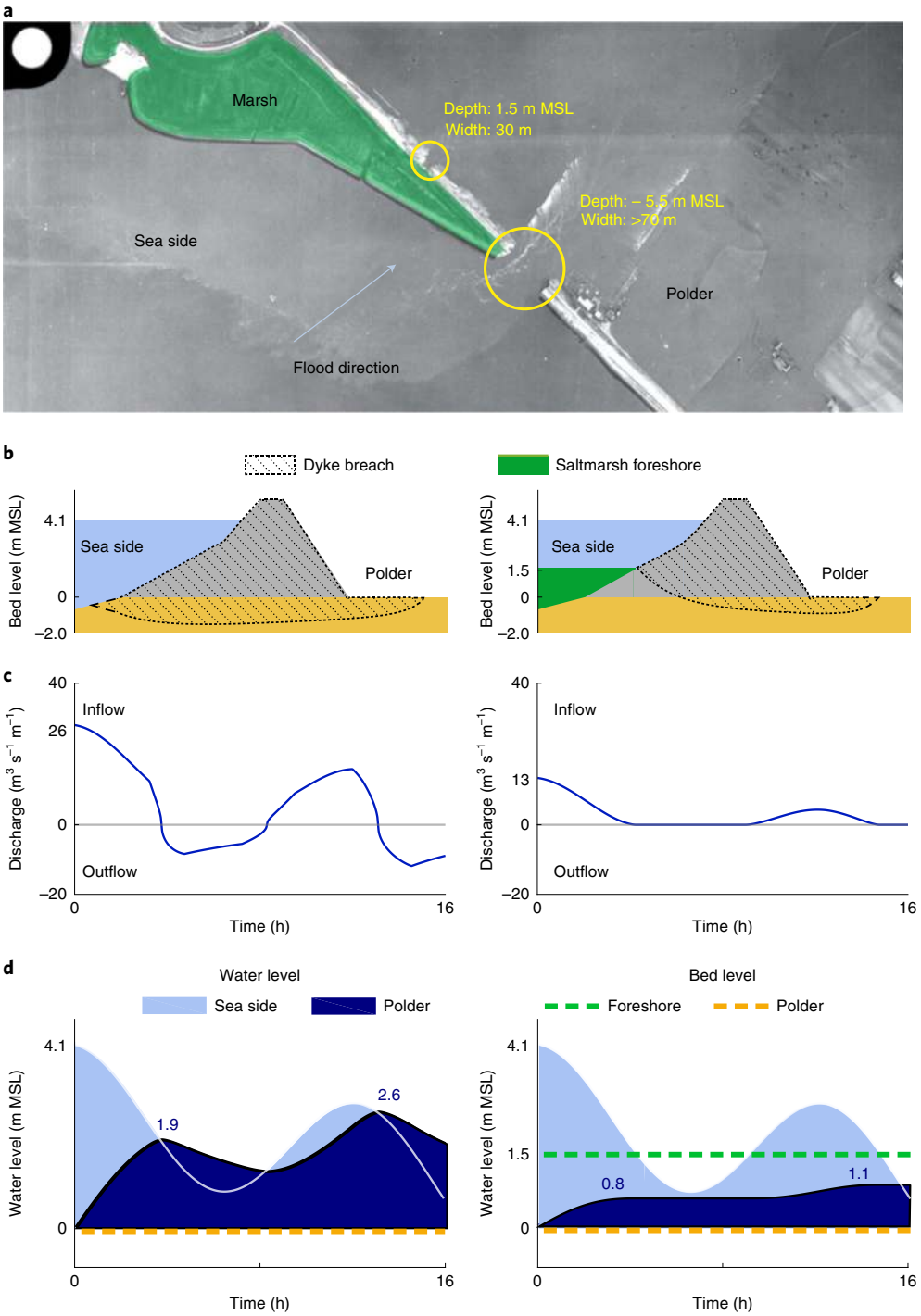

Fig. 4 | Analysis of dyke breach records from the 1953 North Sea flood. a, An aerial image showing two neighbouring dyke breaches in a dyke along the former Dutch estuary Haringvliet. **b**, Illustrations of the difference in sea-side breach depth between the dyke section without (left) and with a saltmarsh foreshore (right). **c**, Difference in breach discharge between these two types of dyke breaches. The breach width was assumed to be identical to allow conservative comparisons. **d**, Consequence for the inundation depth in the area behind the dyke over time. Credit: photo in **a** adapted from Dotka Data B.V.

elevation to the rising sea, they are still much less efficient in reducing the fatality rate than self-adapting marshes when dykes fail (Fig. 5b). This is simply because the elevation of the latter (1.5 m MSL) is higher than the former (0 m MSL). Yet such a difference in elevation (that is, 1.5 m) is not so extreme and can be even larger in many places. For instance, in the Dutch Westerschelde estuary (one of the most affected areas in the 1953 flood), the elevation of marshes fronting the dyke are on average about 2.6 m higher than the bare tidal flats in front of the dyke, and approximately 1.8 m higher than the land behind the dyke (Supplementary Fig. 2).

Implications for developing novel nature-based flood defences

The presented historic lessons demonstrate that nature-based flood defences combining engineered structures and coastal wetlands are actually more advantageous than previously thought. The presence

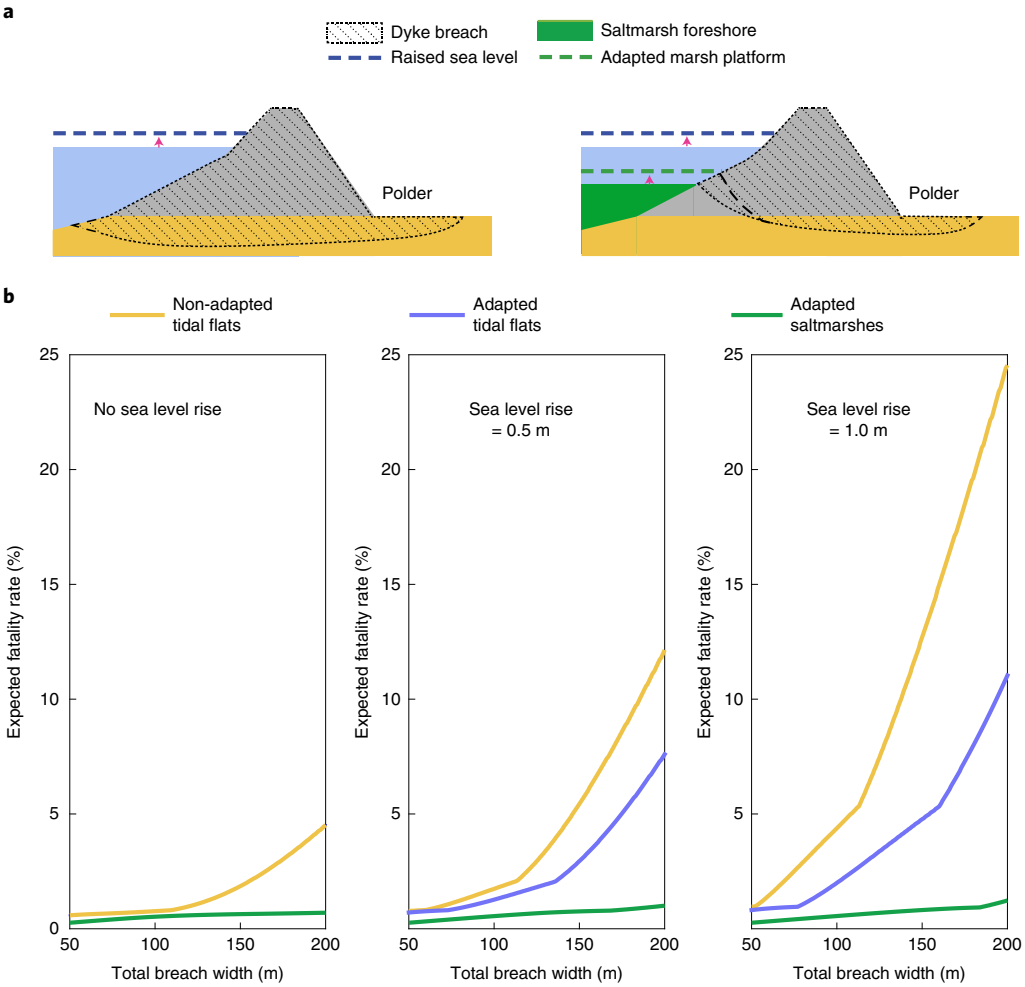

Fig. 5 | Relative advantage of saltmarsh foreshores over tidal flats in reducing flood impact under sea level rise. a, The rising sea level causes higher water depth on the sea side of the dyke without saltmarsh foreshores, whereas it remains unchanged in the presence of a saltmarsh foreshore that can keep pace with the rising sea level. **b**, The calculated fatality rate after dyke failure for three different foreshore scenarios: non-adapted tidal flats, adapted tidal flats and adapted saltmarshes. We assumed no delayed breaching process and no reduced breach width due to wave attenuation by saltmarshes to allow conservative comparisons between saltmarsh foreshores and bare tidal flats.

of saltmarsh foreshores not only reduces the likelihood of dyke failure, but also lowers flood impact by limiting breach dimensions, and continues to do so under sea level rise. Although the latter is only applicable when the inland (polder) area is lower in elevation than the marsh, such a situation is not limited to Northwest Europe, from where the historic evidence comes. Lower inland elevation is also found in other heavily populated low-lying regions, such as the Ganges–Brahmaputra tidal delta[29] and the Mekong delta[30], both located in Asia, where mangroves have similar wave-attenuating and sediment stabilization functions[31]. Moreover, given the accelerating sea level rise and land subsidence, the scenario of low inland elevation is expected to become increasingly common in other large low-lying deltas[32], such as the Mississippi (US), Guayas (Ecuador), Irrawady (Myanmar), Yangtze (China) and Pearl (China) river deltas. Innovative nature-based flood defences combining engineered structures and coastal wetlands will thus become more globally relevant and applicable in the future.

The current study provides new insights into the mechanisms of nature-based flood defences with coastal wetlands: saltmarshes can lower flood depth, and consequently flood damage and casualties, simply by confining dyke breach dimensions. Unlike wave attenuation, this flood defence mechanism is beneficial for both wave-exposed and wave-sheltered locations where engineered structures are needed to mitigate flood risks. This finding reduces the uncertainties in the efficiency of nature-based flood defences: even in situations where the wave dissipation value of the coastal ecosystems is uncertain (for example, due to winter decay or storm damage of above-ground vegetation)[24,33] or not relevant (at wave-sheltered locations), saltmarshes in front of dykes are still highly valuable in coastal defence as they minimize flood impact when a dyke fails. For example, many dykes in wave-sheltered locations were breached by the extreme water level during the 1953 flood[5,6], but saltmarsh foreshores there contributed to limited development of breach depth. This highlights the equal importance of conserving or restoring marshes at wave-sheltered locations as those at wave-exposed sites for enhancing the safety of engineered defences during severe storms.

Our findings greatly broaden the scope of nature-based flood defence approaches. To harness nature's flood protection value, marshes or mangroves ideally have to be preserved or developed on the sea side of the dyke. However, these wetlands may retreat laterally due to wave attack, even if they accrete vertically[34–36], and sea level rise combined with reduced sediment supply may amplify lateral erosion[37,38]. Moreover, physical conditions in front of the

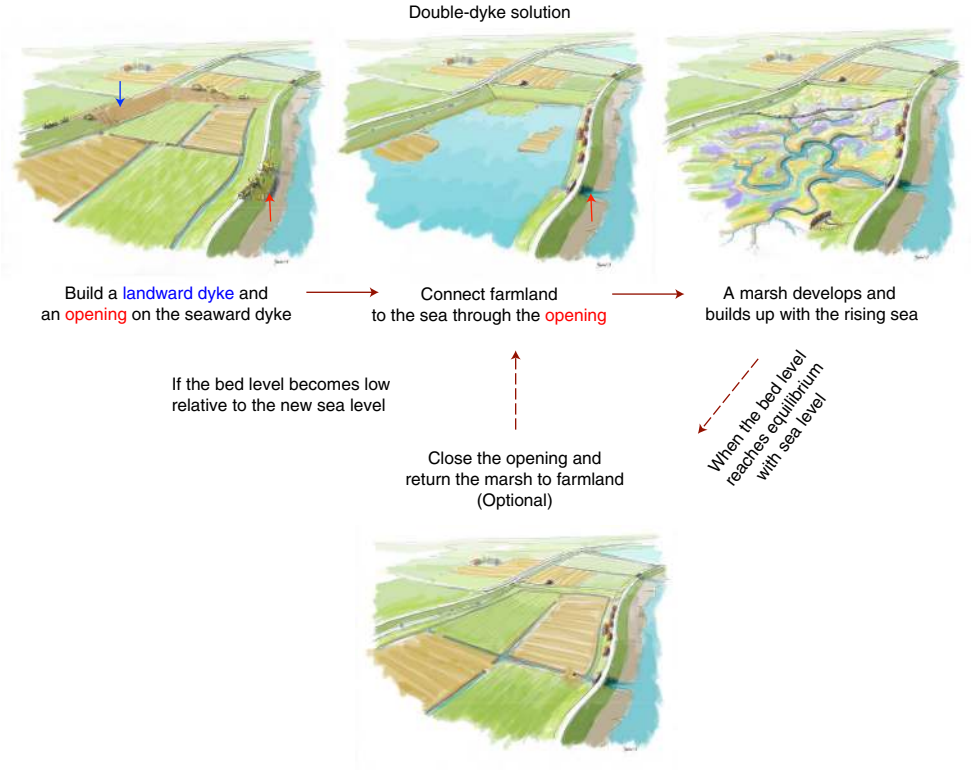

Fig. 6 | An example of steps to implement novel nature-based flood protection with marshes between double dykes. Cartoons are made by an illustrator: Jeroen Helmer/ARK Nature.

dyke are often too harsh for marsh establishment[24,39]. Even in situations where no marshes can exist in front of a dyke, we may still be able to enhance coastal safety by creating saltmarshes in between double dykes. This requires that a secondary, more landward dyke is present and that the more seaward primary dyke is opened to allow tidal flooding, sediment deposition and vertical marsh growth in between the primary and secondary dykes (Fig. 6). Wetlands between double dykes along a river have been used in flood-prone countries such as Belgium (for example, the Sigma Plan) to enhance water storing capacity, thus lowering the water level during extreme events[40]. Present findings indicate that wetland creation between double-dyke systems could also be applied along a seacoast or wide estuary. Such wetlands are not effective in markedly lowering surge levels, given their relatively small water storage capacity as compared with the large volume of the adjacent sea or estuary. They cannot attenuate waves either, as they are located behind a dyke. However, the generally higher elevated wetland surface can greatly lower flood impacts by reducing the breach dimensions, in case the landward secondary dykes should fail. Moreover, self-adapting wetlands that raise elevation by accumulating sediment can strongly buffer the effects of sea level rise, as demonstrated in this study. Once the marsh elevation reaches a balance with the rising sea level, the marsh might be temporarily used again for agriculture, and returned now and then for a period into a wetland that naturally adapts to the rising sea (Fig. 6).

Overall, the current research sheds new light on the mechanisms and benefits of nature-based mitigation of flood hazards, which should stimulate the development of novel hybrid flood defence designs that smartly harness the different flood protection functions of wetlands, as effective adaptive responses to the rising flood risks associated with global change. Large-scale implementation of the current findings first requires further investigation of the global-scale applicability of the findings beyond this study area (the Netherlands) as well as local-scale transdisciplinary efforts to achieve practical implementation by outreach to policymakers and local communities.

Methods

Analysis of the 1717 Christmas flood. The historic map presented in Fig. 1a was produced before 1723 by Barent Heijne, one of the land surveyors hired to estimate the dyke damage during the 1717 flood[25]. An historic report[25] suggests that the survey was conducted on several occasions between January 1718 and September 1718, during which the number of dyke breaches, their widths (measured along the dyke) and the depths of the scour holes were reported. In addition, this report also documents the dimensions of five sections of the seawall depicted on this map (Supplementary Table 2). By the early eighteenth century, land surveyors were technically able to reach a high accuracy for large-scale maps (mapping area $<100\,km^2$) like this one. A study[41] that systematically tested the planimetric accuracy of historic maps between the sixteenth and nineteenth centuries showed that the 'mean positional error' of large-scale maps was 23.3 ± 34.1 m (mean $\pm$ s.d., $n=7$). This accuracy is high when compared with the dyke length (17.5 km in total) and marsh width (0–1.2 km) displayed in this historic map (Fig. 1a). Thus, the accuracy of such maps was already very high in the sixteenth century and did not really improve until the twentieth century[41].

To assess whether the presence of saltmarshes reduced the probability of dyke breaching during this extreme flood, we measured the interval between adjacent dyke breaches and linked it with the corresponding marsh width in front. Because a higher interval of dyke breaches indicates a lower frequency of dyke breaching, we used the inverse of breach interval (that is, we divided the unit dyke length by breach interval) as a proxy for dyke breaching probability. The breach interval was determined as the average distance of a given breach to the adjacent breaches on both sides. This was not done for the breach at either end of the map, as they each have only one neighbouring breach. Nor was this measured for the three mega breaches and the two average breaches next to them, because the locations of these mega breaches are only roughly shown on the map (Fig. 1a). We calculated the breach intervals for the remaining 24 breaches, and related them to the corresponding marsh width, measured as the distance from the centre of the breach to the nearest marsh edge. We measured the marsh width with a ruler and converted it into real dimensions, based on the scale of the map, for which we converted the old Dutch unit 'roede' into 'metre' (1 roede = 4.09 m); 100 roede on the map measures 13.5 mm. The ruler has an accuracy of 0.5 mm, which translates into an accuracy of around 15 m in real dimensions.

We ranked the marsh width and classified the data into three marsh width classes: 0–200, 200–700 and 700–1,200 m (Supplementary Fig. 3). The boundaries

between two classes were set where the differences between two adjacent data points were noticeably larger than between the others. To check whether the positional error of the map may cause considerable changes in the marsh width classification, we conducted a sensitivity analysis by shifting the boundaries by ±57.4 m (that is, the worst-case scenario of the error). The results clearly showed that the shifted boundaries (the blue lines in Supplementary Fig. 3) have no effect on the number of dyke breaches per marsh width class. For each class, we further calculated the number of breaches per unit dyke length and the total breach width per unit dyke length (that is, 1 km). Because the breach width was not available for all individual breaches, the total breach width was determined by multiplying the total number by the average breach width for each class group. The calculation of the average breach width was based on the documented width of 20 breaches (Supplementary Table 1). The three mega breaches were treated as average dyke breaches due to the lack of data on their dimensions, yielding a highly conservative estimation of total breach width for the '0–200 m' marsh width class.

Because dykes failed mainly due to erosion caused by wave overtopping, influenced by water level and wave height[23], we further investigated whether the difference in dyke breaching might be a result of spatial variation of water level and incoming waves. First, we acquired an historic map (Fig. 2a) depicting the coastal geometry of the Dutch Wadden Sea in the 1740s, which is to our knowledge the best one to inform the coastal geometry of the considered area depicted in Fig. 1a. Reconstructing the tidal and wave conditions during the 1717 storm was not possible due to the lack of hydrodynamic and topographic data, however, this map clearly displays uniform tidal flats fronting the marshes and the dyke, similarly to the current configuration (Fig. 2b). This implies no large difference in wave exposure at the marsh edge and the bare tidal flat just in front of the dyke during the 1717 storm as storm waves are limited in height by the water depth in the shallow Wadden Sea. The offshore bathymetric complexity (including barrier islands, tidal inlets, channels and flats) is expected to have minor impacts for the following reasons: (1) waves at the Wadden Sea dykes are dominated by local wind waves, with limited influence from swell waves from the North Sea[42], (2) the large-scale bathymetry of 1717 was not fundamentally different from that of the contemporary situation (the barrier island Schiermonnikoog remains there in the northwest, with tidal inlets found on both sides and uniform tidal flats surrounding the dyke, Fig. 2a) and (3) the influence of offshore bathymetric complexity was probably even smaller in 1717 than it is today, as the dykes were about 1 km further landward in 1717 than in the contemporary situation.

To verify whether water levels and wave heights during severe storm surges are comparable in the case of uniform tidal flats in the considered region, we analysed existing data on peak water levels and significant wave heights (H_{m0}) during modern extreme storm conditions at the marsh edge along the Dutch Wadden Sea coast. This analysis was based on the most recent (2011) official dataset of wave simulations (the interaction with currents was included) for the safety assessment of the Dutch Wadden Sea dykes[43]. The dataset of wave conditions and water levels contains statistical results from a combination of different wave modelling simulations using varying wind conditions. The wave simulations were performed using SWAN[44] and were based on the present-day geometry with a mesh size of approximately 20 m cross-shore and 100 m alongshore[43]. Data for two distinct scenarios, 1-in-100 year and 1-in-3,000 year, were used in our analysis. For each scenario we used 64 data points of H_{m0} along the marsh edge (about 15 km) in the considered district. We also measured the distance from these points to the nearest dyke, that is, the width of the marsh, to determine whether the marsh width is related to H_{m0} at the corresponding marsh edge. Despite the large variation in marsh width, the simulations indicated no large-scale spatial differences in water level and wave exposure at the marsh edge during these extreme storm conditions, regardless of the position relative to the channels or the islands to the north (Supplementary Fig. 1).

Field support from two present-day storms. To examine the relationship between saltmarsh width and wave loads on the dyke, we conducted field observations of waves during two 1-in-5-year storm surges in 2015 and 2017 in a wave-exposed marsh in the same Dutch region (Fig. 3a). This site is characterized by a spatially homogeneous dyke orientation and thereby homogeneous wind exposure, but a short-distance spatial gradient in marsh width. Both the high and low marsh are dominated by couch grass, whereas the pioneer zone is dominated by glasswort and patches of cordgrass. Wave gauges (Ocean Sensor Systems) were deployed at multiple stations (Supplementary Table 4) on the marsh and bare mudflat. Every wave gauge was mounted on a steel pole with the sensor approximately 10 cm above the ground. Using a real-time kinematic global positioning system (RTK-GPS) device (Leica GS12), bed levels next to the wave gauges were measured one day before and ten days after the 2017 storm to quantify the change in bed level during the storm. Earlier post-storm measurements were not possible due to logistical difficulties caused by snow after the storm. Using the RTK-GPS device, the height of each wave gauge was also measured to check their stability during the storm. The results (Supplementary Table 4) showed negligible changes (mean ± s.d., 1 ± 6 mm), implying very stable wave gauges during the storm and an overall high accuracy of elevation measurement. Significant wave heights during the storm were calculated on the basis of pressure signals (see ref. [16] for detailed methods) recorded with a frequency of 5 Hz over a period of 7 min every 15 min in 2015, and continuously in 2017.

The wave run-up height was inferred from the height (m relative to MSL) of the flotsam on the dyke[45,46], measured along the 2-km stretch of dyke behind the foreshore with deployed wave gauges (Fig. 3b). These measurements were performed three days after the storm in 2015 and ten days after the 2017 storm using the RTK-GPS device. To examine the relationship between the wave run-up height and the width of the saltmarsh in front, we also measured the distance from the wave run-up measurement point to the nearest marsh edge. The marsh edge was identified by a sharp drop in both the normalized difference vegetation index and the elevation derived from remote sensing images. We calculated the normalized difference vegetation index from a 2016 colour-infrared aerial image (CIR-LRL) with a ground resolution of 25 cm (source: Waterschapshuis) and used the most recent LIDAR (light detection and ranging)-based digital elevation model (2013) with a ground resolution of 2 m and a vertical accuracy of 5–10 cm (source: Rijkswaterstaat).

Benefits of saltmarshes in mitigating flood magnitude. To illustrate the relative benefit of the typically higher elevated saltmarsh foreshore over bare tidal flats in mitigating flood impacts, we calculated the flow discharge through the breaches (both with and without saltmarshes) and the resultant change in inundation depth in the polder (that is, the low inland area). Because we aimed to demonstrate general principles with typical examples rather than provide accurate calculations of the flooding process, we did this using a simple one-dimensional model that captures the key parameters (including breach width, bed level in front of the dyke breach and that behind the breach). Specifically, we applied the geometric characteristics of the two contrasting dyke breaches (Fig. 4a) during the 1953 flood on the northern shore of the Haringvliet estuary (Supplementary Fig. 4; this estuary has been closed since 1970). For the sake of simplicity and to allow conservative comparisons, we applied an identical breach width ($W = 70$ m) and assumed that breaching occurs at the same time (during peak water levels) for the two breach types. In reality, reduced wave forcing by saltmarshes can slow down the dyke breaching process and limit the total width of dyke breaches (Fig. 1b).

The flow discharge (Q) is estimated using the expression $Q = UWh$, where W is the breach width measured along the dyke, U is the flow velocity in the breach and h is the upstream water depth. The value of h is determined by the local water level ζ and the breach depth z_b, that is, the bed level on the upstream edge of the breach. For the breach that occurred behind the marsh foreshore, z_b is the elevation of the marsh near the dyke (1.5 m MSL). Without saltmarsh, we assume z_b to be the bed level on the land side of the dyke (0 m MSL), which was 1.5 m lower than the marsh but higher than the tidal flat in front of the dyke (Fig. 4b). Data from a reliable report on the 1953 storm[5] were used to characterize the time-varying local water level (tide and surge) in the Haringvliet estuary, with a peak water level of 4.1 m MSL and a tidal amplitude of 1.9 m. Flow can be either critical or subcritical, depending on the water level difference over the breach. Critical flow occurs when only the water depth limits the flow velocity. The inflow causes rising water levels in the polder. When the difference in water level between both sides of the breach diminishes, the flow becomes subcritical. The flow velocity is calculated using $U = \sqrt{gh}$ for critical flow and $U = C\sqrt{Ri}$ for subcritical flow, where g is the gravitational acceleration, C is the Chézy roughness coefficient, set to 45 $m^{0.5}$ s^{-1}, R is the hydraulic radius of the breach and i is the water level gradient based on an assumed width of 100 m over which the water level difference exists. Subcritical flow has little effect on the results, as the flow through the breach is critical most of the time.

The inundation depth in the polder (d) was computed using $d = V/S$, where V is the water volume entering the polder and S is the surface area of the polder. V is calculated from the inflow and outflow discharge over time. We adopted a value of 10 km^2 for S, which is approximately the actual surface area of the polder behind the two breaches in Fig. 4a.

Benefits of saltmarshes in mitigating flood impact under sea level rise. We further examined the relative benefit of saltmarsh foreshores over tidal flats in reducing flood impact under sea level rise. To achieve this, we computed the expected fatality rate based on the inundation depth and water level rise rate, which were found to be two key factors determining the number of deaths during many floods[28,47,48]. Specifically, we examined how the expected fatality rate during coastal flooding (1) varies with changing total breach width, (2) responds to sea level rise and (3) differs between three foreshore scenarios, namely adapted saltmarshes, adapted tidal flats and non-adapted tidal flats. We did not include the scenario of non-adapted saltmarshes, as recent studies have concluded that most marshes are able to build up their elevation with the rising sea when provided with sufficient sediment[18,19].

For each scenario, we first calculated the time series inundation depth in the polder for the two dyke breaching types. We used the same geometric characteristics and methods as described above, but with changing mean sea level and varying total breach width. We assumed no delayed breaching process and no reduced breach width due to wave attenuation by saltmarshes to allow conservative comparisons. To simulate different sea level rise scenarios, we adjusted the value of the breach depth (z_b, bed level of the breach) according to the change in mean sea level. For the scenarios of adapted saltmarshes and adapted tidal flats, z_b is set to remain unchanged (1.5 and 0 m MSL, respectively). For the scenario

of non-adapted tidal flats, the bed level (m MSL) in front of the dyke becomes relatively lower due to the raised mean sea level. In this case, we calculated z_b by subtracting the magnitude of sea level rise (R_{sl}) from the the initial value (0 m MSL). For R_{sl}, we adopted two distinct values, 50 and 100 cm, given the predicted range (28–98 cm) of global mean sea level rise by 2100 according to the latest IPCC report[49]. We additionally adopted a value of 0 for R_{sl} to generate a blank control. For the breach behind the marsh foreshore, z_b was left unchanged (1.5 m MSL) due to the vertical adaptability of the saltmarsh platform by sediment accumulation[15,18,19]. For both breach types, the bed level (m MSL) of the flooded area, that is, the polder, becomes relatively lower due to the raised mean sea level. Similarly, the dyke height above the mean sea level also becomes lower. We assumed no increase in the chance of dyke breaching due to relatively lower dyke height under sea level rise to produce a conservative estimation. For each scenario, we used the same tide and storm surge height above the mean sea level, but varied the value of total breach width from 50 to 200 m to check the sensitivity of the results to the magnitude of the breach width. We applied the same value of total breach width for the two breach types to allow a conservative comparison between them.

For each combined scenario of breach type, breach width and sea level rise, we derived the maximum inundation depth (d) based on the time series inundation depth computed for the period of the first 16 h after breaching, during which the inundation depth peaked twice due to the tidal cycle (Fig. 4d). Because a rapid water level rise only occurred in the initial stage, we used the first peak water depth to determine the water rise rate (w). The value of w is calculated by dividing this peak depth by the time it took to reach it. The expected fatality rate was then calculated using the interpolated fatality functions based on the 1953 floods in the Netherlands[28,47,48]. Here, fatality rate (F) is described as a lognormal function of d and w, with the values of the parameters varying with the flooding conditions that characterize three different zones:

(1) Fatality rate in the zone with rapidly rising waters ($d \geq 2.1$ m and $w \geq 4$ m h^{-1})

$$F_{\mathrm{Rise}}(d) = \Phi_{\mathrm{N}}\left(\frac{\ln(d)-\mu_{\mathrm{N}}}{\sigma_{\mathrm{N}}}\right)$$
$$\mu_{\mathrm{N}} = 1.46 \qquad \sigma_{\mathrm{N}} = 0.28$$

(2) Fatality rate in the remaining zone ($d < 2.1$ m and $w < 0.5$ m h^{-1})

$$F_{\mathrm{Remain}}(d) = \Phi_{\mathrm{N}}\left(\frac{\ln(d)-\mu_{\mathrm{N}}}{\sigma_{\mathrm{N}}}\right)$$
$$\mu_{\mathrm{N}} = 7.60 \qquad \sigma_{\mathrm{N}} = 2.75$$

(3) Fatality rate in the transition zone ($d \geq 2.1$ m and $0.5 \leq w < 4$)

$$F = F_{\mathrm{Remain}} + (w - 0.5)\frac{F_{\mathrm{Rise}} - F_{\mathrm{Remain}}}{3.5}$$

Statistics. Linear regressions were employed to detect whether there were statistically significant relationships between the interval between dyke breaches and the corresponding width of the saltmarsh in front, and between the wave run-up height on the dyke and the marsh width in front. Prior to the analysis, data normality was checked through Shapiro–Wilk tests[50]. Where needed, the data were log transformed to improve data normality. All the statistical analyses were performed in R (https://www.r-project.org/), applying a significance level of $\alpha = 0.05$.

Reporting Summary. Further information on research design is available in the Nature Research Reporting Summary linked to this article.

Data availability

The collected wave data for the two present-day storms are available on figshare (https://doi.org/10.6084/m9.figshare.6011129.v2). Other data that support the findings of this study are available within the paper and its supplementary information files.

Code availability

The Matlab scripts for calculating breach discharge and the expected fatality rate in the flooded area are available on figshare (https://doi.org/10.6084/m9.figshare.6010958).

Received: 16 October 2019; Accepted: 21 May 2020;
Published online: 29 June 2020

References

1. Barbier, E. B. A global strategy for protecting vulnerable coastal populations. *Science* **345**, 1250–1251 (2014).
2. Hallegatte, S., Green, C., Nicholls, R. J. & Corfee-Morlot, J. Future flood losses in major coastal cities. *Nat. Clim. Change* **3**, 802–806 (2013).
3. Blake E. S., Rappaport E. N. and Landsea C. W. *The Deadliest, Costliest, and Most Intense United States Tropical Cyclones from 1851 to 2006 (and other frequently requested hurricane facts)* (National Oceanic and Atmospheric Administration/National Weather Service, National Centers for Environmental Prediction, National Hurricane Center, 2007).
4. Nakamura, R., Shibayama, T., Esteban, M. & Iwamoto, T. Future typhoon and storm surges under different global warming scenarios: case study of typhoon Haiyan (2013). *Nat. Hazards* **82**, 1645–1681 (2016).
5. Rijkswaterstaat & KNMI *Verslag over de Stormvloed van 1953* (Staatsdrukkerij, 1961).
6. Gerritsen, H. What happened in 1953? The Big Flood in the Netherlands in retrospect. *Philos. Trans. R. Soc. A* **363**, 1271–1291 (2005).
7. Jakubowski-Tiessen, M. *Sturmflut 1717: die Bewältigung einer Naturkatastrophe in der frühen Neuzeit* (Oldenbourg, 1992).
8. Lamb, H. & Frydendahl, K. *Historic Storms of the North Sea, British Isles and Northwest Europe* (Cambridge Univ. Press, 1991).
9. Wahl, T. et al. Understanding extreme sea levels for broad-scale coastal impact and adaptation analysis. *Nat. Commun.* **8**, 16075 (2017).
10. IPCC *Special Report on Global Warming of 1.5 °C* (eds Masson-Delmotte, V. et al.) (WMO, 2018).
11. Syvitski, J. P. M. et al. Sinking deltas due to human activities. *Nat. Geosci.* **2**, 681–686 (2009).
12. Neumann, B., Vafeidis, A. T., Zimmermann, J. & Nicholls, R. J. Future coastal population growth and exposure to sea-level rise and coastal flooding - a global assessment. *PLoS ONE* **10**, e0118571 (2015).
13. Cheong, S.-M. et al. Coastal adaptation with ecological engineering. *Nat. Clim. Change* **3**, 787–791 (2013).
14. Temmerman, S. et al. Ecosystem-based coastal defence in the face of global change. *Nature* **504**, 79–83 (2013).
15. Temmerman, S. & Kirwan, M. L. Building land with a rising sea. *Science* **349**, 588–589 (2015).
16. Vuik, V., Jonkman, S. N., Borsje, B. W. & Suzuki, T. Nature-based flood protection: the efficiency of vegetated foreshores for reducing wave loads on coastal dikes. *Coast. Eng.* **116**, 42–56 (2016).
17. Barbier, E. B. et al. The value of estuarine and coastal ecosystem services. *Ecol. Monogr.* **81**, 169–193 (2011).
18. Kirwan, M. L., Temmerman, S., Skeehan, E. E., Guntenspergen, G. R. & Fagherazzi, S. Overestimation of marsh vulnerability to sea level rise. *Nat. Clim. Change* **6**, 253–260 (2016).
19. Kirwan, M. L. & Megonigal, J. P. Tidal wetland stability in the face of human impacts and sea-level rise. *Nature* **504**, 53–60 (2013).
20. Moller, I. et al. Wave attenuation over coastal salt marshes under storm surge conditions. *Nat. Geosci.* **7**, 727–731 (2014).
21. Arkema, K. K. et al. Coastal habitats shield people and property from sea-level rise and storms. *Nat. Clim. Change* **3**, 913–918 (2013).
22. Narayan, S. et al. The value of coastal wetlands for flood damage reduction in the northeastern USA. *Sci. Rep.* **7**, 9463 (2017).
23. Visser, P. J. *Breach Growth in Sand-Dikes*. PhD thesis, Delft Univ. Technology (1998).
24. Bouma, T. J. et al. Identifying knowledge gaps hampering application of intertidal habitats in coastal protection: opportunities & steps to take. *Coast. Eng.* **87**, 147–157 (2014).
25. Seeratt, T. V. *Journaal van de Commies Provinciaal Thomas van Seeratt Betref de Dijken over de Jaren 1716–1721* Archive no. 818 (Groninger Archives, 1730).
26. Willemsen, P. W., Borsje, B. W., Vuik, V., Bouma, T. J. & Hulscher, S. J. Field-based decadal wave attenuating capacity of combined tidal flats and salt marshes. *Coast. Eng.* **156**, 103628 (2020).
27. Spencer, T. et al. Salt marsh surface survives true-to-scale simulated storm surges. *Earth Surf. Process. Landf.* **41**, 543–552 (2016).
28. Jonkman, S. N., Bočkarjova, M., Kok, M. & Bernardini, P. Integrated hydrodynamic and economic modelling of flood damage in the Netherlands. *Ecol. Econ.* **66**, 77–90 (2008).
29. Auerbach, L. W. et al. Flood risk of natural and embanked landscapes on the Ganges–Brahmaputra tidal delta plain. Nat. *Clim. Change* **5**, 153–157 (2015).
30. Minderhoud, P. S. J., Coumou, L., Erkens, G., Middelkoop, H. & Stouthamer, E. Mekong delta much lower than previously assumed in sea-level rise impact assessments. *Nat. Commun.* **10**, 3847 (2019).
31. Van Coppenolle, R., Schwarz, C. & Temmerman, S. Contribution of mangroves and salt marshes to nature-based mitigation of coastal flood risks in major deltas of the world. *Estuar. Coast.* **41**, 1699–1711 (2018).
32. Van Coppenolle, R. & Temmerman, S. A global exploration of tidal wetland creation for nature-based flood risk mitigation in coastal cities. *Estuar. Coast. Shelf Sci.* **226**, 106262 (2019).
33. Vuik, V., van Vuren, S., Borsje, B. W., van Wesenbeeck, B. K. & Jonkman, S. N. Assessing safety of nature-based flood defenses: dealing with extremes and uncertainties. *Coast. Eng.* **139**, 47–64 (2018).
34. Schuerch, M., Spencer, T. & Evans, B. Coupling between tidal mudflats and salt marshes affects marsh morphology. *Mar. Geol.* **412**, 95–106 (2019).
35. Wiberg, P. L., Fagherazzi, S. & Kirwan, M. L. Improving predictions of salt marsh evolution through better integration of data and models. *Annu. Rev. Mar. Sci.* **12**, 389–413 (2020).

36. Leonardi, N., Ganju, N. K. & Fagherazzi, S. A linear relationship between wave power and erosion determines salt-marsh resilience to violent storms and hurricanes. *Proc. Natl Acad. Sci. USA* **113**, 64–68 (2016).
37. Mariotti, G. & Fagherazzi, S. A numerical model for the coupled long-term evolution of salt marshes and tidal flats. *J. Geophys. Res. Earth Surf.* **115**, F01004 (2010).
38. Ladd, C. J., Duggan-Edwards, M. F., Bouma, T. J., Pagès, J. F. & Skov, M. W. Sediment supply explains long-term and large-scale patterns in salt marsh lateral expansion and erosion. *Geophys. Res. Lett.* **46**, 11178–11187 (2019).
39. Friess, D. A. et al. Are all intertidal wetlands naturally created equal? Bottlenecks, thresholds and knowledge gaps to mangrove and saltmarsh ecosystems. *Biol. Rev.* **87**, 346–366 (2012).
40. Vandenbruwaene, W. et al. Sedimentation and response to sea-level rise of a restored marsh with reduced tidal exchange: comparison with a natural tidal marsh. *Geomorphology* **130**, 115–126 (2011).
41. Jongepier, I., Soens, T., Temmerman, S. & Missiaen, T. Assessing the planimetric accuracy of historical maps (sixteenth to nineteenth centuries): new methods and potential for coastal landscape reconstruction. *Cartogr. J.* **53**, 114–132 (2016).
42. Groeneweg, J. et al. Wave modelling in a tidal inlet: performance of SWAN in the Wadden Sea. In *Coastal Engineering 2008: Proc. 31st International Conference on Coastal Engineering* (ed. Smith, J. M.) 411–423 (World Scientific, 2009).
43. Groeneweg, J., Beckers, J. & Gautier, C. A probabilistic model for the determination of hydraulic boundary conditions in a dynamic coastal system. In *Coastal Engineering 2010: Proc. 32nd International Conference on Coastal Engineering* (eds Smith, J. M. & Lynett, P.) (ICEE, 2011).
44. Booij, N., Ris, R. & Holthuijsen, L. H. A third-generation wave model for coastal regions: 1. model description and validation. *J. Geophys. Res. Oceans* **104**, 7649–7666 (1999).
45. Niemeyer, H. D., Kaiser, R. & Berkenbrink, C. Increased overtopping security of dykes: a potential for compensating future impacts of climate change. In *Coastal Engineering 2010: Proc. 32nd International Conference on Coastal Engineering* (eds Smith, J. M. & Lynett, P.) (ICEE, 2011).
46. Grüne, J. Evaluation of wave climate parameters from benchmarking flotsam levels. In *Proc. International Conference on Coastlines, Structures and Breakwaters* (ed. Allsop, N. W. H.) 468–477 (Thomas Telford Publishing, 2005).
47. Jonkman, S. N. *Loss of Life Estimation in Flood Risk Assessment: Theory and Applications*. PhD thesis, Delft Univ. Technology (2007).
48. Jonkman, S. N., Vrijling, J. K. & Vrouwenvelder, A. C. W. M. Methods for the estimation of loss of life due to floods: a literature review and a proposal for a new method. *Nat. Hazards* **46**, 353–389 (2008).
49. IPCC *Climate Change 2013: The Physical Science Basis* (eds Stocker, T. F. et al.) (Cambridge Univ. Press, 2014).
50. Shapiro, S. S. & Wilk, M. B. An analysis of variance test for normality (complete samples). *Biometrika* **52**, 591–611 (1965).

Acknowledgements

We thank I. Kratzer and J. de Smit for their help in the field. We also thank A. Wielemaker for GIS support and Q. Zhu for the assistance in polishing the figures. This work is part of the research programme BESAFE, financed by the Netherlands Organization for Scientific Research (NWO). Additional financial support has been provided by Deltares, Boskalis, Van Oord, Rijkswaterstaat, World Wildlife Fund, HZ University of Applied Science and ARK Natuurontwikkeling. Z.Z. was also supported by the project funded by the China Postdoctoral Science Foundation (2019M652825) and the Key Special Project for Introduced Talents Team of the Southern Marine Science and Engineering Guangdong Laboratory (Guangzhou; GML2019ZD0403).

Author contributions

Z.Z., V.V., S.T. and T.J.B. conceived the idea for the paper and wrote the initial draft. Z.Z., V.V., T.S., P.J.V. and S.N.J. collected and analysed the data. All authors discussed the results and improved on the manuscript.

Competing interests

The authors declare no competing interests.

Additional information

Supplementary information is available for this paper at https://doi.org/10.1038/s41893-020-0556-z.

Correspondence and requests for materials should be addressed to Z.Z.

Reprints and permissions information is available at www.nature.com/reprints.

Publisher's note Springer Nature remains neutral with regard to jurisdictional claims in published maps and institutional affiliations.

nature research

Corresponding author(s): Zhenchang Zhu

Last updated by author(s): Feb 11, 2020

Reporting Summary

Nature Research wishes to improve the reproducibility of the work that we publish. This form provides structure for consistency and transparency in reporting. For further information on Nature Research policies, see Authors & Referees and the Editorial Policy Checklist.

Statistics

For all statistical analyses, confirm that the following items are present in the figure legend, table legend, main text, or Methods section.

n/a	Confirmed	
☐	☒	The exact sample size (*n*) for each experimental group/condition, given as a discrete number and unit of measurement
☐	☒	A statement on whether measurements were taken from distinct samples or whether the same sample was measured repeatedly
☒	☐	The statistical test(s) used AND whether they are one- or two-sided *Only common tests should be described solely by name; describe more complex techniques in the Methods section.*
☒	☐	A description of all covariates tested
☐	☒	A description of any assumptions or corrections, such as tests of normality and adjustment for multiple comparisons
☐	☒	A full description of the statistical parameters including central tendency (e.g. means) or other basic estimates (e.g. regression coefficient) AND variation (e.g. standard deviation) or associated estimates of uncertainty (e.g. confidence intervals)
☒	☐	For null hypothesis testing, the test statistic (e.g. *F*, *t*, *r*) with confidence intervals, effect sizes, degrees of freedom and *P* value noted *Give P values as exact values whenever suitable.*
☒	☐	For Bayesian analysis, information on the choice of priors and Markov chain Monte Carlo settings
☒	☐	For hierarchical and complex designs, identification of the appropriate level for tests and full reporting of outcomes
☒	☐	Estimates of effect sizes (e.g. Cohen's *d*, Pearson's *r*), indicating how they were calculated

Our web collection on statistics for biologists contains articles on many of the points above.

Software and code

Policy information about availability of computer code

Data collection	N/A
Data analysis	We used R (version 3.53) for statistical analysis, and Matlab (2014b) for calculating breach discharge and the fatality rate for different scenarios.

For manuscripts utilizing custom algorithms or software that are central to the research but not yet described in published literature, software must be made available to editors/reviewers. We strongly encourage code deposition in a community repository (e.g. GitHub). See the Nature Research guidelines for submitting code & software for further information.

Data

Policy information about availability of data

All manuscripts must include a data availability statement. This statement should provide the following information, where applicable:

- Accession codes, unique identifiers, or web links for publicly available datasets
- A list of figures that have associated raw data
- A description of any restrictions on data availability

The Matlab scripts for calculating breach discharge and the expected fatality rate in the flooded area are available on figshare (https://doi.org/10.6084/m9.figshare.6010958.v5).The collected wave data for the two present-day storms are available on figshare (https://doi.org/10.6084/m9.figshare.6011129.v2). Other data that support the findings of this study are available within the paper and its supplementary information files.

Field-specific reporting

Please select the one below that is the best fit for your research. If you are not sure, read the appropriate sections before making your selection.

☐ Life sciences ☐ Behavioural & social sciences ☒ Ecological, evolutionary & environmental sciences

For a reference copy of the document with all sections, see nature.com/documents/nr-reporting-summary-flat.pdf

Ecological, evolutionary & environmental sciences study design

All studies must disclose on these points even when the disclosure is negative.

Study description	1. We analyzed historic dike breaching records (breach number and breach width) during 1717 flood and related it to the marsh width in front of the dike. 2. In the field, we measured wave run up on the dike during two storms and related it to marsh width in front of the dike. 3. We analyzed the characteristics of breach dimensions for all dike breaches in the primary dikes in the Netherlands during the 1953 flood. 4. Based on 3, we modeled the relative advantage of saltmarsh foreshore over tidal flats in mitigating flood impacts after dike breaching with a 1D model that captures the key parameters (including breach width, bed level in front of the dike breach and that behind the breach)
Research sample	For the analysis of the relationship between breach number (or total breach width) and marsh width, we used all relevant data available on the historic map (Fig. 1a) and in the reports (ref 5 and 25). For wave run up on the dike, we measured the positions of flotsam materials for multiple locations (n>10) along the 2km dike (Fig. 3b). All dike breaches in the primary dikes in the Netherlands during the 1953 flood were used to detect the characteristics of breach depth for different foreshore types.
Sampling strategy	For the historic data, we used all available data from the map and associated reports. For the measurements of wave run-up, we collected the data from random points (at least 10m apart), along the 2km dike section.
Data collection	Dike breaching records and associated marsh width data during the 1717 flood were obtained from the historic map map (Fig. 1a, source: Amsterdam, Historisch Archief Waterschap Amstel, Gooi en Vecht, Beeldbank Toegang 80, Kaart 020478; https://www.archieven.nl) and report (ref 25). Zhenchang Zhu measured marsh width in front of each dike breach, calculated dike breaching interval and total breach width per unit dike length for different marsh width class. Zhenchang Zhu and Vincent Vuik did the wave run-up measurement along the 2 km dike (Fig. 3b) using a DGPS. Paul Visser analzed the dike breaching records in a report (ref 5) for the 1953 flood.
Timing and spatial scale	Timing and spatial scale was not relevant for the analysis of historic dataset. Measurement of wave run-up during the storm was done three days after the storm in 2015 and 10 days after the 2017 storm along the 2 km dike behind the foreshore with deployed wave gauges.
Data exclusions	The calculation of dike breach interval was not done for the two breaches on each of the map ends as they only have one neighboring breach depicted in the map. Nor was this measured for three mega breaches (written as 'met meyvelt gelyck' on the map) and the two average breaches next to them, since the locations of these mega breaches were only roughly shown in the map
Reproducibility	Measurement of wave run-up on the dike during the storm was done for two storms at the same site to verify the reproducibility.
Randomization	Wave run-up measurements were done at random locations along the 2 km dike behind the foreshore with deployed wave gauges.
Blinding	Blinding was not relevant for this study, as the data used here had no 'identity' to hide.

Did the study involve field work? ☒ Yes ☐ No

Field work, collection and transport

Field conditions	The field measurement was conducted in winter (January). The temperature and precipitation was not relevant for our wave measurments.
Location	A marsh along the Wadden Sea coast of the Netherlands (Coordinates: 6.66 E, 53.46 N)
Access and import/export	This site is accessible to anyone
Disturbance	No disturbance in our case

Reporting for specific materials, systems and methods

We require information from authors about some types of materials, experimental systems and methods used in many studies. Here, indicate whether each material, system or method listed is relevant to your study. If you are not sure if a list item applies to your research, read the appropriate section before selecting a response.

Materials & experimental systems

n/a	Involved in the study
☒	☐ Antibodies
☒	☐ Eukaryotic cell lines
☒	☐ Palaeontology
☒	☐ Animals and other organisms
☒	☐ Human research participants
☒	☐ Clinical data

Methods

n/a	Involved in the study
☒	☐ ChIP-seq
☒	☐ Flow cytometry
☒	☐ MRI-based neuroimaging